Charles Baylis, Matthew Fellows, Matthew Flachsbart, Jennifer Barlow, Joseph Barkate, and Robert J. Marks.
``Enabling the Internet of Things: Reconfigurable power amplifier techniques using intelligent algorithms and the Smith tube.''
In Circuits and Systems Conference (DCAS), 2014 IEEE Dallas, pp. 1-4. IEEE, 2014.

Enabling the Internet of Things: Reconfigurable Power Amplifier Techniques Using Intelligent Algorithms and the Smith Tube

Charles Baylis, Matthew Fellows, Matthew Flachsbart, Jennifer Barlow, Joseph Barkate, and Robert J. Marks II

Wireless and Microwave Circuits and Systems Program
Department of Electrical and Computer Engineering
Baylor University
Waco, TX, USA

***Abstract*—Future Internet of Things (IoT) devices will need to maintain high power efficiency while being able to reconfigure for changing performance requirements and operating frequencies. The design of quickly reconfigurable power amplifiers able to maintain high efficiency and meet spectral requirements will be critical to success. This paper discusses fast optimization techniques that will be useful in real-time optimization of transmitter power amplifiers: (1) a vector-based algorithm to find the load impedance giving the highest power-added efficiency (PAE) while keeping the adjacent-channel power ratio (ACPR) below a prespecified minimum, (2) the use of a spectral mask directly in the load-pull optimization in place of the ACPR, and (3) the extension of the Smith Chart to a three-dimensional, cylindrical "Smith Tube" for optimization involving an additional parameter: the waveform bandwidth. This paper builds a framework for design and the real-time optimization of reconfigurable, efficient, and spectrally compliant IoT power amplifiers.**

***Topic Areas*—electronics for infrastructure systems, low-power design, communications, reconfigurable systems**

I. Introduction

The recent momentum in constructing the Internet of Things (IoT) will require a significant amount of devices using the radio spectrum. In a recent paper, Palattella identifies power efficiency as an important criterion for the IoT, and also pinpoints power amplifiers as a source of significant power expenditure in the system [1]. Because IoT systems often must operate in multiple protocols and standards, flexibility in operating frequency is useful [2]. Because of the large number of simultaneous spectrum users expected, each user's transmission and reception will be required to operate within a stringent spectral mask. These demands require reconfigurable power amplifiers optimizable for power efficiency and spectral compliance.

The spectral spreading of a transmitter's power amplifier is based on its linearity. The linearity/efficiency tradeoff is important, as designers desire to maximize the power efficiency while minimizing the spectral spreading related to nonlinearities. Both the power-added efficiency (PAE) and adjacent-channel power ratio (ACPR) are dependent upon the transistor load impedance. In the literature, the ACPR has been connected with the third- and fifth-order intermodulation products in the nonlinear amplifier [3]. Sechi delineates a method to find the Pareto-optimal load impedance for third-order intermodulation (IM3) and efficiency, solving a similar problem, from pre-measured load-pull data [4]. While this approach is very useful in optimizing this important design tradeoff, it does not improve the swiftness of the load-pull, and therefore makes it difficult for implementation in a real-time reconfigurable transmitter. If a system is reconfiguring in real-time, it must find the optimum load impedance with as few measurements as possible. Impedance tuning algorithms prove useful for this purpose, and many have been suggested by the literature, including genetic algorithms [5, 6], fuzzy control [7], neural networks [8], and least-squares optimization [9]. Real-time load-impedance tuning [10] and reconfigurable matching networks [11] have been suggested and demonstrated in the literature as a way to provide desired impedance-dependent behavior. A recent paper by Cui demonstrates a power amplifier specifically for IoT application with a dual-band, reconfigurable matching network [2]. Other issues related to amplifiers and the IoT are also described in the literature [12, 13, 14, 15].

The focus of this paper is to overview several recent innovations from our group that will be useful in creating quickly reconfigurable circuitry to facilitate the IoT.

II. Fast Load-Pull for the PAE/ACPR Tradeoff

The PAE/ACPR tradeoff is of significance in amplifier operation for the IoT. The leakage into the adjacent channel is limited by practical or regulatory limitations based on coexistence considerations. For example, Figure 1 shows measured load-pull data for a Skyworks packaged amplifier

978-1-4799-5924-2/14/$31.00 ©2014 IEEE

excited by a broadband frequency-modulation (FM) signal, where the ACPR is required to be below -27.5 dBc. It is desirable to select the load reflection coefficient Γ_L that maximizes the PAE while constraining the ACPR to lie within the "Acceptable Terminations Region" (possessing ACPR less than a pre-specified maximum) shown in Fig. 1. However, an IoT device cannot spend the time to characterize each state in a full load-pull for "on-the-fly" reconfiguration.

An algorithm created by our group for the purpose of changing power amplifier load impedance in real-time [16] can be applied to reconfiguring IoT power amplifiers. This algorithm allows reconfiguration to precisely optimize PAE while keeping within ACPR requirements in a small number of measurements. Figure 2 shows the basic concept behind this vector-based load-pull search.

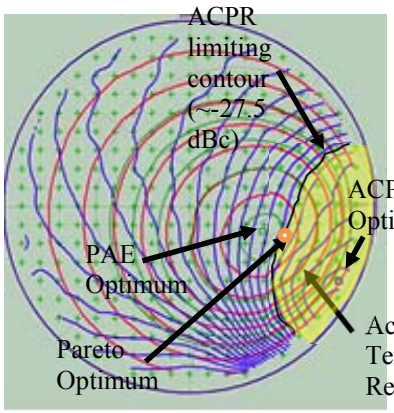

Fig. 1. Measured PAE (red) and ACPR (blue) load-pull contours for a Skyworks packaged amplifier with broadband signal excitation. The region of acceptable terminations meeting the PAE and ACPR requirements is shown (similar to [18]).

As explained in [16], the search is conducted using search vectors. A starting value for the load reflection coefficient Γ_L is specified by the user. From this point, two measurements are made at points slightly above and to the right of the candidate on the Smith chart, as shown in Fig. 3. This allows estimation of the PAE gradient and ACPR gradient. The unit vector in the direction of the PAE gradient is given as $\hat{p}$ and the unit vector opposite to the direction of the ACPR gradient is given as $\hat{a}$. The unit-vector bisector between these vectors is $\hat{b}$. The next candidate is selected using these vectors and the user-specified search distance D_s. When the ACPR value is above the acceptable limit, the following equations are used to calculate the vector $\bar{v}$ to the next candidate [16]:

$$\bar{v} = \hat{a}D_a + \hat{b}D_b \tag{1}$$

where

$$D_a = \frac{D_s}{2}\frac{|ACPR_{meas} - ACPR_{target}|}{|ACPR_{worst} - ACPR_{target}|} \tag{2}$$

and

$$D_b = \frac{D_s}{2}\frac{|\theta_{meas} - \theta_{target}|}{\theta_{target}} \tag{3}$$

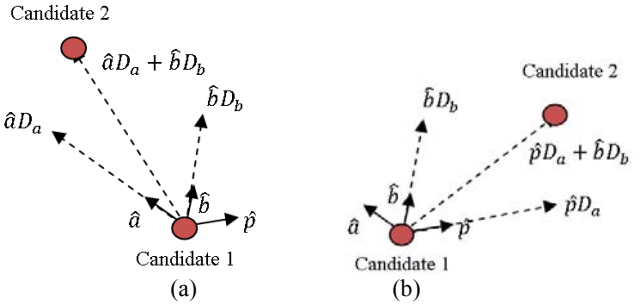

Fig. 2. Schematic of vector-based load-pull search behavior (a) when the ACPR at Candidate 1 is not within limitations and (b) when the ACPR at Candidate 1 is within limitations, reprinted from [12].

θ is the angle between $\hat{b}$ and $\hat{a}$ and guides the search toward the tradeoff line between PAE and ACPR, or the locus of *Pareto optimum solutions*. On the Pareto optimum locus, the gradients are oppositely directed and $\theta = \theta_{target} = 90°$. The value of $ACPR_{target}$ is equal to the ACPR limit imposed based on spectral regulations.

If the ACPR value is within the acceptable limit, the vector to the next candidate is instead given by

$$\bar{v} = \hat{p}D_a + \hat{b}D_b \tag{4}$$

The value of D_s is divided by three when (1) the search is inside the ACPR acceptable region and attempts to leave or (2) the search is inside the ACPR acceptable region and a new candidate point gives a lower value of PAE, as described in [16]. In both of these cases, the search returns to the previous candidate and performs another attempt.

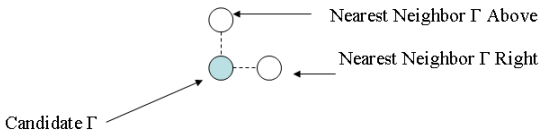

Fig. 3. Measurements to estimate the PAE and ACPR gradients and calculate $\hat{a}$ and $\hat{p}$. Reprinted from [16].

A more detailed presentation of the results from this search algorithm is presented in [16]. Bench-top testing of this new algorithm was performed (the laboratory measurement setup is shown in Fig. 4). It can be seen in Fig. 5 that accurate results are obtained with the fast search, requiring only 17 measurements. The reflection-coefficient value providing the best compromise between PAE and ACPR can be found to high precision with only about 20 measurement queries. This is very useful for real-time optimization, and this technique will also speed the design process, allowing quick performance of load-pull characterization measurements for different power levels, bias settings, and frequencies. This will allow the PA design process to be much more effective and efficient.

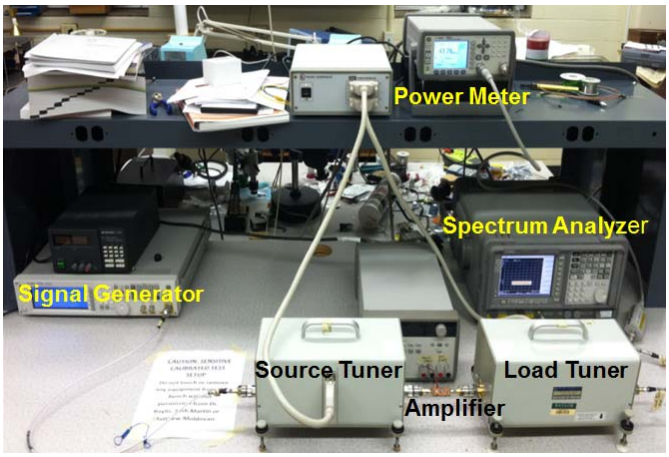

Fig. 4. Measurement test bench

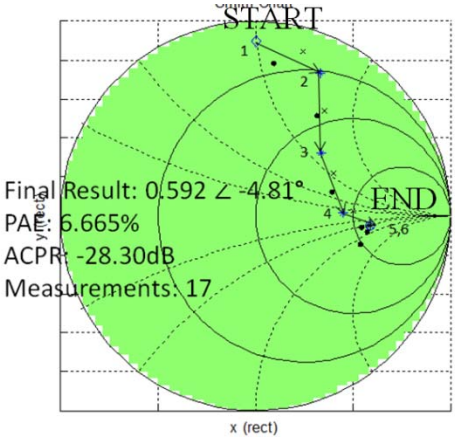

Fig. 5. Sample fast load-pull search results starting from $\Gamma_L = 0.9$ /-90°, reprinted from [16]. Only 17 measured values of Γ_L were required to find the optimum in this fast load-pull.

III. Finding the Load Termination Based on Spectral-Mask Compliance

It may be more useful to examine and optimize the transmitter spectral compliance directly by the spectral mask for the optimization. ACPR, while useful for measuring the linearity of the device, does not provide a concrete indication of spectral mask compliance. We have developed an approach geared toward the real-time optimization of radar transmitters that also applies to the load-pull based design of nonlinear power amplifiers for communications and radar applications alike [17]. The metric S_m, describing the maximum distance between the spectrum and the spectral mask, can be used rather than ACPR for the linearity optimization [17]:

$$S_m = \max(s - m) \tag{5}$$

In this equation, s is the power in dBm of the measured power spectrum, and m is the power of the spectral mask level in dBm. When the spectrum is in compliance with the spectral mask, the value of S_m is less than or equal to zero. The vector-based algorithm from the search using PAE and ACPR was adapted to use S_m instead of ACPR. As in the previous algorithm, this search can find the value of Γ_L providing the highest PAE while meeting spectral mask requirements ($S_m \leq 0$) with a small number of measurements. Figure 6 shows measurement results of the PAE-and-S_m load-pull search using the Skyworks amplifier. An optimum was obtained using only 10 measurements, maximizing the PAE while keeping S_m below zero. This type of load-pull allows an intelligent, measurement-based search that is based *directly* on the spectral mask.

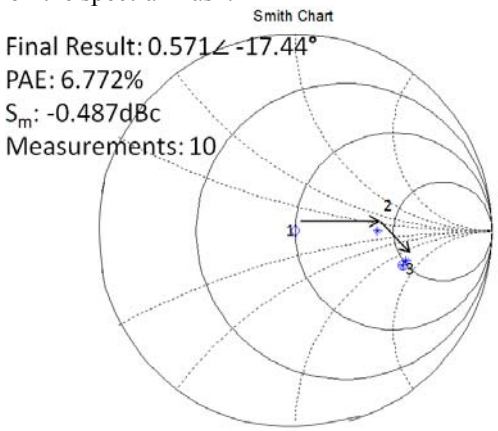

Fig. 6. PAE-and-S_m load-pull measurement search algorithm results starting from $\Gamma_L = 0$, reprinted from [17].

IV. The Smith Tube for Matching Network and Bandwidth Design

We have demonstrated a design procedure to include both the load reflection coefficient Γ_L and the waveform bandwidth B by extending the Smith chart cylindrically into a third dimension. The Smith Tube (Fig. 7), as introduced in [18], provides a three-dimensional search space where these three parameters can be jointly designed.

The vertical axis of the Smith Tube represents the adjustable bandwidth of a waveform. In designing for the IoT, it is often desirable to maximize the bandwidth to increase the data rate. However, PAE and spectral mask (or ACPR) requirements must also be met by the system. Figure 8 shows the design of the Skyworks packaged amplifier load reflection coefficient and bandwidth to find the highest bandwidth where ACPR ≤ -27.5 dBc and PAE ≥ 7%, as described in [18]. The optimum is the highest point in the intersection of the PAE and ACPR acceptable regions [18].

V. Conclusions

Internet of Things device design requires flexibility to meet changing requirements in power efficiency, data rate, and spectrum performance. This paper shows recently developed algorithms for power amplifier circuit and waveform optimization that could prove useful to reconfigure circuits for IoT transmitters. Recently developed algorithms can quickly optimize multiple conflicting criteria in a real-time reconfigurable power amplifier with a small number of measurements. Joint PAE/ACPR optimizations, a spectral mask metric, and the Smith Tube are useful tools for real-

time reconfiguration of load reflection coefficient and for joint design of the circuit and transmission waveform.

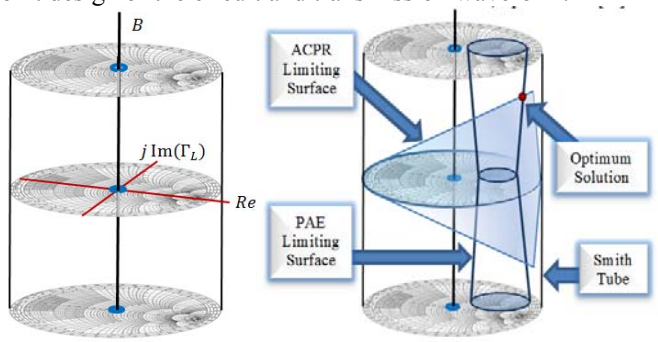

(a) (b)

Fig. 7. (a) The Smith Tube, reprinted from [15]. The vertical axis represents an additional parameter (possibly chirp bandwidth *B*), and the horizontal cross section of the tube is a Smith chart. (b) Conceptual drawing of the Smith Tube solution of the radar bandwidth design problem, reprinted from [15]. The optimum point provides the largest bandwidth possible while meeting the PAE and ACPR requirements.

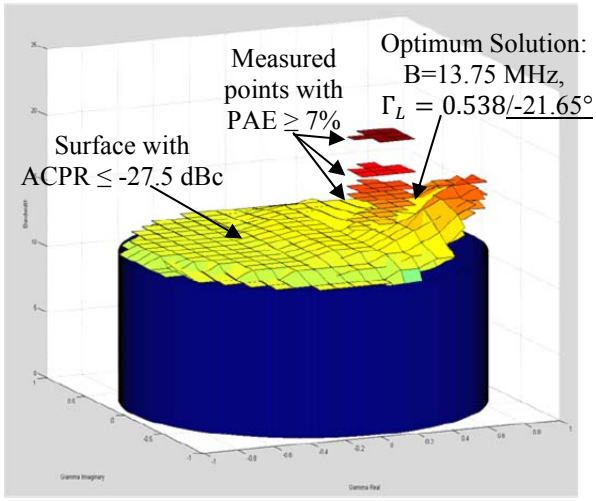

Fig. 8. Surfaces representing the locus of points shown in the Smith tube with ACPR = -27.5 dBc and PAE = 7.0%. The optimum solution is the highest intersection of the PAE and ACPR surfaces. Reprinted from [14].

ACKNOWLEDGMENTS

The authors wish to thank Lawrence Cohen of the U.S. Naval Research Laboratory for his collaboration and valuable contributions to this paper. This work has been funded by a grant from the National Science Foundation (NSF) (Award No. ECCS-1343316).

REFERENCES

[1] M.R. Palattella, N. Accettura, X. Vilajosana, T. Watteyne, L.A. Grieco, G. Boggia, and M. Dohler, "Standardized Protocol Stack for the Internet of (Important) Things," *IEEE Communications Surveys & Tutorials*, Vol. 15, Issue 3, July 2013, pp. 1389-1406.

[2] J. Cui, K. Zhang, T. Tian, "A Dual-Level and Dual-Band Class-D CMOS Power Amplifier for IoT Applications," 2013 IEEE 11th International New Circuits and Systems Conference, Paris, France, June 2013.

[3] Q. Wu, H. Xiao, and F. Li, "Linear Power Amplifier Design for CDMA Signals: A Spectrum Analysis Approach," *Microwave Journal*, 1998.

[4] F.N. Sechi, "Design Procedure for High-Efficiency Linear Microwave Power Amplifiers," *IEEE Transactions on Microwave Theory and Techniques*, Vol. 28, Pt. 1, November 1980, pp. 1157-1163.

[5] Y. Sun, "Evolutionary Tuning Method for Automatic Impedance Matching in Communication Systems," Proceedings of the 1998 IEEE International Conference on Electronics, Circuits, and Systems, Vol. 3, pp. 73-77.

[6] Y. Sun and W.K. Lau, "Antenna Impedance Matching Using Genetic Algorithms," Proceedings of the IEE Conference on Antennas and Propagation, York, United Kingdom, August 1999, pp. 31-36.

[7] E. Arroyo-Huerta, A. Diaz-Mendez, J. Ramirez Cortes, and J. Garcia, "An Adaptive Impedance Matching Approach Based on Fuzzy Control," 52nd IEEE International Midwest Symposium on Circuits and Systems, August 2009, pp. 889-892.

[8] J. Hemminger, "Antenna Impedance Matching with Neural Networks," *International Journal of Nerual Systems* (IJNS), Vol. 15, No. 5, pp. 357-361, 2005.

[9] A. Mushi, D. Johns, and A. Sedra, "Adaptive Impedance Matching," proceedings of the IEEE International Symposium on Circuits and Systems, 1994 (ISCAS '94), Vol. 2, pp. 69-72.

[10] Y. Sun, J. Moritz, and X. Zhu, "Adaptive Impedance Matching and Antenna Tuning for Green Software-Defined and Cognitive Radio," 54th IEEE International Midwest Symposium on Circuits and Systems, 2011, pp. 1-4.

[11] M. Fellows, M. Flachsbart, J. Barlow, C. Baylis, and R.J. Marks II, "The Smith Tube: Selection of Radar Chirp Waveform Bandwidth and Power Amplifier Load Impedance Using Multiple-Bandwidth Load-Pull Measurements," IEEE Wireless and Microwave Technology Conference (WAMICON 2014), Tampa, Florida, June 2014.

[12] C. Li, M. Li, K. Khalaf, A. Bourdoux, M. Verhelst, M. Ingels, P. Wambacq, J. Craninckx, L. Van Der Perre, and S. Pollin, "Opportunities and Challenges of Digital Signal Processing in Deeply Technology-Scaled Transceivers." *Journal of Signal Processing Systems,* 2014, pp. 1-15.

[13] S. Balasubramanian, S. Boumaiza, H. Sarbishaei, T. Quach, P. Orlando, J. Volakis, G. Creech, J. Wilson, and W. Khalil, "Ultimate Transmission." *IEEE Microwave Magazine,* Vol. 13, No. 1, January 2012, pp. 64-82.

[14] M. Li, K. Khalaf, C. Li, V. Vojkan, M. Ingels, A. Bourdoux, P. Wambacq, J. Craninckx, and L. Van der Perre, "Signal Processing Challenges for Emerging Digital Intensive and Digitally Assisted Transceivers with Deeply Scaled Technology." 2013 IEEE Workshop on Signal Processing Systems (SiPS), pp. 324-329.

[15] J. Xia, S. Garg, and S. Boumaiza, "A Hybrid Amplitude/Time Encoding Scheme for Enhancing Coding Efficiency and Dynamic Range in Digitally Modulated Power Amplifiers." *IEEE Journal on Emerging and Selected Topics in Circuits and Systems*, Vol. 3, No. 4, December 2013, pp. 498-507.

[16] M. Fellows, C. Baylis, J. Martin, L. Cohen, and R.J. Marks II, "Direct Algorithm for the Pareto Load-Pull Optimisation of Power-Added Efficiency and Adjacent-Channel Power Ratio," Accepted October 2013 for publication in *IET Radar, Sonar & Navigation*.

[17] M. Fellows, C. Baylis, L. Cohen, and R.J. Marks II, "Real-Time Load Impedance Optimization for Radar Spectral Mask Compliance and Power Efficiency," Accepted for publication in *IEEE Transactions on Aerospace and Electronic Systems*, September 2014.

[18] M. Fellows, M. Flachsbart, J. Barlow, C. Baylis, and R.J. Marks II, "The Smith Tube: Selection of Radar Chirp Waveform Bandwidth and Power Amplifier Load Impedance Using Multiple-Bandwidth Load-Pull Measurements," 2014 IEEE Wireless and Microwave Technology Conference, Tampa, Florida, June 2014.

[19] M. Fellows, M. Flachsbart, J. Barlow, J. Barkate, C. Baylis, L. Cohen, and R.J. Marks II, "Fast, Combined Optimization of Chirp Waveform Bandwidth and Power Amplifier Load Impedance for Real-Time Reconfigurable Radar," Submitted to *IEEE Transactions on Aerospace and Electronic Systems*, May 2014.